STUDY OF THE REACTION MECHANISMS OF BENZALDEHYDE HYDROGENATION OVER Cu-Fe-LDH LIKE-HYDROTALCITE AND DERIVED MIXED OXIDES

[1]HANANE ZAZOUA, [2]IBTISSEM LOUNAS, [3]ADEL SAADI, [4]KHALDOUN BACHARI

[1,2,3] Laboratory of Natural Gas Chemistry, Faculty of Chemistry, University of Science and Technology Houari Boumediene (USTHB), Algiers, Algeria
[1,4] Environmental Chemistry Division, Scientific and Technical Research Center in Physico-Chemical Analysis (CRAPC), Tipaza, Algeria
E-mail: [1]hanene_zazoua@yahoo.fr, [2] ibtissem.lounas@gmail.com, [3] adel_saadi@yahoo.fr, [4]bachari2000@yahoo.fr.

Abstract - The catalytic activity Cu-Fe-LDH hydrotalite-like compound and their precursors calcined as heterogeneous catalyst was investigated at atmospheric pressure in the gaseous phase benzaldehyde hydrogenation. Hydrotalcite precursor Cu-Fe-LDH was prepared by co-precipitation method with Cu^{2+}/Fe^{3+} molar ratio of ~ 2 at pH=10 using carbonates as an interlayer anions and Cu/Fe-HT mixed oxides were prepared by calcinations of Cu-Fe-LDH at different temperatures (400, 600 and 800°C). The catalytic performance of catalysts sensitive on both reaction temperature and the nature of oxides formed after the heat-treatment. The maximum of conversion was observed at 200°C for Cu-Fe-800, such high catalytic efficiency could reasonably be attributed to the presence of both Cu^{2+} and Fe^{3+} ions in the octahedral sites of the ferrite sub-lattice and active metallic copper species, which controlled the key to hydrogenation related to the adsorption of benzaldehyde molecules and following activation of carbonyl groups and the dissociation of hydrogen.

Keywords: Hydrotalcite; Copper; Iron; Hydrogenation; Benzaldehyde; Benzyl alcohol.

I. INTRODUCTION

Layered double hydroxydes or hydrotalcite-like compounds are class of two-two-dimensional (2D) anionic lamellar materials characterized by a stack of sheets brucite-like. The chemical composition can be represented by the general formula: $[M(II)_{1-x}M(III)_x(OH)_2]^{x+}(A^{n-})_{x/n}.mH_2O$[1,2], where M^{2+} is a bivalent cation (Mg^{2+}, Co^{2+}, Ni^{2+}, Zn^{2+}, Mn^{2+}, Cd^{2+}), M^{3+} is a trivalent cation (Al^{3+}, Fe^{3+}, Cr^{3+}, Ga^{3+}), A^{n-} is an anion (CO_3^{2-}, NO_3^-, Cl^- etc.) [3] and x is defined as the $M^{3+}/[M^{2+}+M^{3+}]$ ratio, whose value varies between 0.2 and 0.4 [4], which occupy the space between the layers compensating for the positive charge and inducing stability in the overall structure[5,6]. The divalent metal cations have been substituted by trivalent ions to form positively charged sheets, where metal cations occupy the centers of octahedra whose vertices are hydroxide ions. These octahedra are connected to each other by edge sharing to form an infinite sheet [7,8]. The cationic charge created in the layers is compensated by the presence of hydrated anions and water molecules present between the stacked sheets.

LDH-based materials are very interesting systems due to their structural peculiarities; brucite-like sheets consisted by different metal cations, adjustable chemical composition layer/interlayer, the compensation of the positive charge of the brucite like sheets by different interlayer anions, opened structure which can accommodate large anionic molecules, and adjustable textural properties controlled by the synthesis process and conditions. All the above physical and chemical properties render the LDH as important class of layered materials with numerous potential applications as catalysts [9], catalyst supports, ion exchanger/adsorbents [10,11], layered hosts for bio-molecules and precursors for composite materials [12], photocatalytic hydrogen production [13], can be potential candidates to catalyze the reaction of benzaldehyde hydrogenation [14].

The hydrogenation of benzaldehyde provides industrially important product, benzyl alcohol is used as intermediate in the synthesis of pharmaceuticals, flavour, fragrances, chemical intermediates and photographic chemicals [15,16]. It is also used as raw material in the manufacture of various esters, such as benzyl formate, acetate, propionate, and butyrate, which are extensively used in the flavour and fragrance industries [17]. The hydrogenation of benzaldehyde is a reaction complex, with two competing hydrogenations of aromatic ring and carbonyl group occurring. Benzaldehyde hydrogenation can be achieved either through phase transfer catalysis [18], hydrogenation by hydrogen transfer [19] or homogeneous catalysis [20].

At present, heterogeneous catalysts are frequently used in this kind of reaction owing to easy product separation and catalyst recycling. Noble metals (Pd, Pt, Rh and Ru) and transition metals (Cu, Co and Ni) are generally selected as catalysts for hydrogenation because; they have characteristic ability towards hydrogen adsorption [21]. Supported Cu catalysts have attracted the researcher's interest due to the low cost of copper. It was found that Cu supported on reducible oxides (CeO_2 and Fe_2O_3) are considered as suitable candidate to hydrogenate the C = O bond due to the presence of metal-support interfacial sites

resulting from the presence of (Ce^{4+}/Ce^{3+} or Fe^{2+}/Fe^{3+}) [22].

This present manuscript is devoted to structure-reactivity studies of Cu-Fe-LDH hydrotalite-like compound and their precursors calcined related to its catalysis performances. It was shown that the bimetallic Cu-Fe catalysts exhibited a substantially enhanced hydrogenation activity as a result the reason of synergistic effect between copper and iron in the tested reaction. The main section of this review gives an overview of the different mechanisms of reaction.

II. DETAILS EXPERIMENTAL

1.1. Catalysts preparation

Co-precipitation at constant pH is the most straightforward and frequently used method for LDH synthesis [23]. This synthesis process is the reaction between two aqueous solutions, one containing nitrate salts as such $Fe^{3+}/[Cu^{2+}+Fe^{3+}] = 0.33$, and the other containing a mixture of $NaOH(1N)/Na_2CO_3(0.25N)$, were added dropwise and the pH at approximately 10 by adjusting the flow of this solution. The suspension thus obtained was kept at 60°C for 15 h. The precipitate was filtered and washed with deionised water until pH~ 7 of the filtrate and then dried at 70°C for 24h. Cu/Fe-HT_S were prepared by calcination of Cu/Fe-LDH. The samples were heated at constant heating rate of 5 °C min^{-1} up to 400, 600 and 800 °C, assigned as Cu/Fe-400, Cu/Fe-600 and Cu/Fe-800, respectively, maintained at this temperature for 4 h and then cooled down to room temperature.

2.2. Precursors characterization

The chemical composition and scanning electron microscopy (SEM) of the catalysts was determined by EDX FEI QUANTA F Environmental apparatus equipped a back-scatter detector (BSE) at 15 kV. Thermal gravimetric analyzer allows analysis of weight changes of sample during temperature increase caused by oxidation and decomposition. The thermal gravimetric analyzer (STA 6000) supplied by Perkin Elmer was used to measure the weight loss of hydrotalcite sample as a function of temperature. Thermogravimetric curve was recorded by heating from 30 to 900°C at 20°C/min in air atmosphere. The thermogravimetric analysis (TGA) was carried out on a Perkin Elmer (STA 6000 with the heating rate of 10 °C min^{-1} under controlled atmosphere (air, N_2).

The crystallization phase of hydrotalcite and the metal oxides obtained were studied using powder X-ray diffraction (PXRD). The analysis was carried out in a Siemens D-5000 diffractometer with a monochromator, using CuKα radiation (λ = 0.154056 nm) over a range of 5–70° (2θ), with step of 0.05° and 2 s by step. The Infra-red spectra were obtained using FTIR spectrophotometer (Alpha Bruker FTIR). Samples were prepared by mixing the powdered solids with potassium bromide, KBr (the blank) in 15:85 ratio to get transparent pellet auto supported on the different solids at 10 ton pressure. The infrared spectra were recorded both over the wave number range from 4000 to 400 cm^{-1}.

Temperature-programmed reduction (TPR) was used to evaluate the relative ease of reduction of sample and detection is done via TCD detector. H_2-TPR of the catalyst was performed using a Micromeritics Auto Chem II 2920 equipped with a thermal conductivity detector (TCD). A 50 mg catalyst sample was reduced in a gaseous mixture of 10% H_2– 90% Ar at a flow rate of 30 ml min^{-1} (at 25 °C; 1 atm) in a heating process at a rate of 10 °C min^{-1}. The textural characteristics, such as BET specific area, pore volume and average pore diameter (BJH method) were determined using conventional nitrogen adsorption/desorption method at -196°C in a Micromeritics Tristar 3000. Prior to nitrogen adsorption, the samples were outgassed for 8 h at 80°C to evacuate the physically adsorbed moisture. Transmission electron microscopy (SEM) experiment was performed on a JEOL 1200 EX II microscope with an acceleration voltage of 120 kV. The samples were dispersed in ethanol, and carbon-coated copper grids were used as the sample holder.

2.3. Catalytic testing

The catalytic performances were carried out in a fixed-bed glass tubular reactor with 0.1 g samples at atmospheric pressure and the total flow rate of 50 $cm^3.min^{-1}$. The reactant gas feed consisted of 4.8 Torr of benzaldehyde (Aldrich, 99.98%) and 250 Torr of H_2 diluted in N_2. Gaseous benzaldehyde was obtained by bubbling N_2 in liquid benzaldehyde maintained at constant temperature (50°C) in a suitable saturator. Before testing, the catalysts were in-situ reduced for 2 h at 350°C in a current of H_2 with a flow rate of 20 $cm^3.min^{-1}$.

The gaseous reactant and products were heated upstream and out stream and analyzed on line by a FID gas chromatograph (Delsi IGC 121 ML) equipped with a 10% CP-SIL 8 CB/ Chromosorb W column. Each reaction temperature was maintained constant until the corresponding steady-state was reached as indicated by the gas chromatograph analysis of the exit gases samples. The catalysts were tested at 100°C and 200°C.

III. RESULTS AND DISCUSSION

3.1. Characterization

The stœchiometry of the synthesized LDH was verified by the MET/EDX analysis. The molar fraction of the cations Cu^{2+}/Fe^{3+} in sheet are reported in table 1. As it can be seen, the Cu^{2+}/Fe^{3+} atomic ratio was similar to that expected. This result confirms that the precipitation process is effective, and indicates that Cu-Fe-HDL sample with Cu^{2+}/Fe^{3+} atomic ratio of 2:1 are successfully prepared by co-precipitation method.

Sample	Cu-Fe-LDH
Theorical ratio Cu^{2+}/Fe^{3+}	2
Cu^{2+}/Fe^{3+} molar ratio	1.80
Cu^{2+}/ Fe^{3+} molar ratio	0.35
d_{003} (Å)	7.836
a (Å)	3.068
c (Å)	23.508
Taille des cristallites (nm)	46

Table.1 Chemical composition and structural parameters of Cu-Fe-LDH

The TG profile of Cu-Fe-LDH indicates two major weight losses of 20% in the first step up to 350°C and that of 8% in the second step between 350 and 700°C, and the DTA profile shows three endothermic peaks at 100, 250 and 650°C (Fig.1). The presence of the two events at temperature below 500 °C are attributed to dehydration of various water molecules (physically adsorbed, crystalline, and H-bound water in the interlayer) and dehydroxylation of OH groups as well as decomposition of interlayer anions in the LDH lattice. The endothermic DTA peak above 500°C is due to decarbonation of interlayer carbonate anions as CO_2, and the formation of oxides phases.

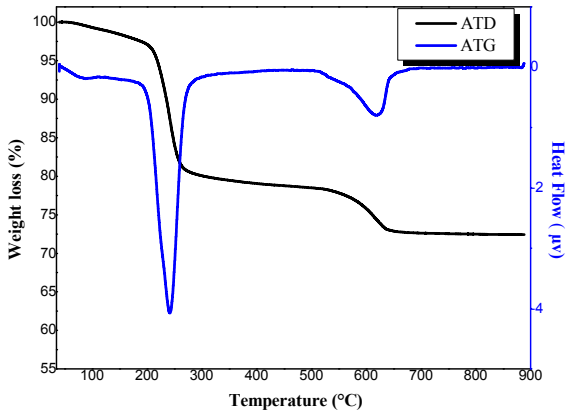


Fig. 1. TG and DTA curves for Cu-Fe-LDH sample

The powder X-ray diffraction patterns (PXRD) of Cu-Fe-LDH and the precursors calcined at different temperatures (400, 600 and 800°C) are shown in Fig.2. The diffractogram of Cu-Fe-LDH exhibited the characteristic basal reflections of hydrotalcite-like LDH composites. At low values of 2θ (11-23°), the result show that diffractogram exhibited sharp and symmetric reflections of (003) and (006) planes and at higher values of 2θ (34-66°), broad and asymmetric reflections of (012), (015) and (018) planes, characteristic of a highly crystalline layered double hydroxide (LDH) structure. These reflections are typical characteristics of the hydrotalcite and revealed a good dispersion of copper and iron in the brucite layers [24]. Presence of CO_3^{2-} anions in the interlayer space of LDH was confirmed by the characteristic basal spacing of (003) plane of sample (d_{003} = 7.65 A°). The values of unit cell parameters (a and c) of Cu-Fe-LDH were calculated by the formula: $a=2(d_{110})$ and $c=3(d_{003})$ [25]; where d_{110} and d_{003} are the basal spacing values of (110) and (003) planes respectively. The parameter "a" is linked to the cation-cation distance within the brucite-like layer while the parameter "c" gives the combined thickness of the brucite-like layer and the interlamellar space. The Cu-Fe-LDH has the "a" unit cell parameter close to that of the natural hydrotalcite (3.05 A°) [24].

After calcination the Cu-Fe-HT at different temperature (400, 600 and 800°C), the reflections corresponding to layered structure completely disappear and new reflections appear (Fig.2). The typical peaks indexed with 2θ approximately at 33°, 38°, 48°, 53°, 58° and 61°,which were attributed of CuO phase (JCPDS 05-0661) whereas those at 2θ= 35°, 56°, 62°,66° and 68° indicate that metallic Fe_2O_3 (JCPDS 39-1346). The typical peaks of spinel $CuFe_2O_4$ (JCPDS 34-0425) with 2θ appearing approximately at 30°, 35° and 62°.When calcinations temperature reaches 800°C, the peaks are most intense among and became sharper the other precursors (Fig.2d), suggesting a higher crystallinity are obtained with small crystal.

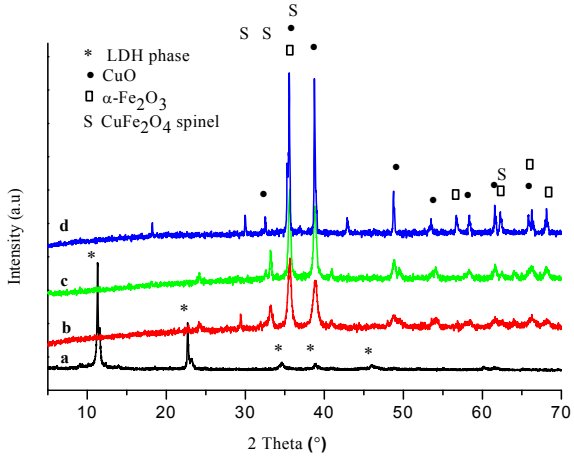


Fig.2. XRD patterns for (a) Cu-Fe-LDH, (b) Cu-Fe-400, (c) Cu-Fe-600 and (d) Cu-Fe-800

FTIR spectra of the Cu-Fe-LDH synthesized and the precursors calcined at different temperatures (400, 600 and 800°C) are shown in Fig.3. The characteristic bands of hydrotalcite-type compound are similar to those of the literature [26] (Fig. 3a). The broad band observed in the 4000-3000 cm^{-1} range is attributed to the O–H stretching mode (νO–H). The OH groups are present in the layers and also in both adsorbed and interlamellar water.

The IR band at about 1643 cm^{-1} is assigned to HOH deformation mode (δH–O–H), thus confirming the presence of water molecules in the interlayer region of the parent materials and that observed at approximately 1384 cm^{-1} to the ν_3 (asymmetric stretching mode) of carbonate anions [27]. The two weak vibration bands located at about 1055 and 843 cm^{-1} were identified as the ν_2 [out-of-plane deformation mode] of carbonate [28].

The FTIR spectra of the precursors calcined were shown in Fig.3 Firstly, increase in temperature decreases the intensity of the IR bands at 1600 and 3500 cm^{-1}(Fig.3d), this result is consistent with the transformation from LDH to mixed oxides carried out through thermal decomposition, involving a number of competing reactions such as dehydration, decomposition of interlayer anions, and dehydroxylation of layer hydroxide. Further, IR spectroscopy shows the new vibration bands in the 800-400 cm^{-1} wavelength regions, see figure 1d. It is remarkable that a new band centered near 600 cm^{-1} appears and the variation in both the intensity and frequency of the new bands is concomitant with increasing calcination temperature, which indicates the formation of oxides phases, this is confirmed by DRX.

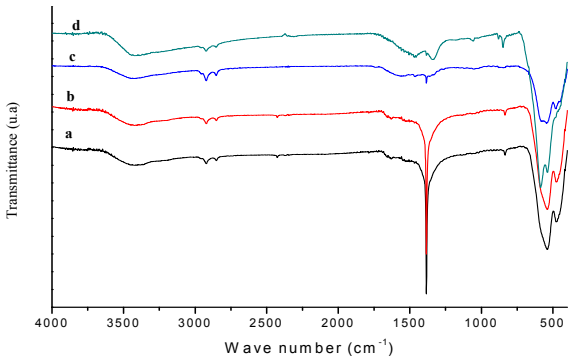


Fig. 3. FT-IR spectra of (a) Cu-Fe-LDH, (b) Cu-Fe-400, (c) Cu-Fe-600 and (d) Cu-Fe-800

The reduction profile of Cu-Fe-LDH measured by H_2-TPR was presented in Fig.4. The reduction of Cu-Fe-HDL showed two distinct reduction events, the peaks appearing in the temperature range of 350-400°C corresponded to the reduction of Cu^{2+} to metallic Cu^0 [29], and at high temperature (400-600°C) event which corresponded to the reduction of Fe^{3+} to metallic Fe^0 [30].

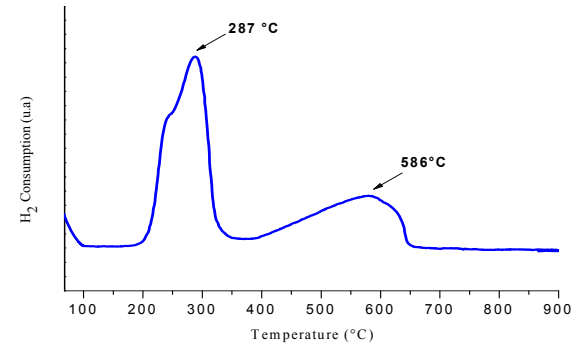


Fig. 4. H_2-TPR profile of the Cu-Fe-LDH sample

The physical properties of the Cu-Fe-LDH synthesized and the precursors Cu-Fe-HTs calcined were evaluated by BET and by N_2 adsorption/desorption measurements, and the results are listed in Table 2. As can be seen, S_{BET} decreases gradually with increasing the calcination temperature; the areas of the calcined hydrotalcites ranged from 3 to 17 m^2g^{-1}. This result can be related to the higher crystallization of the precursors calcined with higher particle size, as it was revealed by XRD.

Sample	BET surface area (m^2/g)	Langmuir surface area (m^2/g)	BJH pore volume (cm^3/g)	BJH pore size (nm)
Cu-Fe-LDH	29	42	0.045	10
Cu-Fe-400	17	23	0.067	17
Cu-Fe-600	9	13	0.022	12
Cu-Fe-800	3	4	-	-

Table 2. BET and Langmuir surface area, BJH pore volume and pore size of the samples

Fig.5 shows the N_2 adsorption-desorption of isotherm graphic and average pore size distribution of Cu-Fe-LDH and calcined precursors. Based on the IUPCA classification, the isotherm of the samples is type IV with the small adsorption at lower P/P_0 values and present a H_3-type hysteresis loops characteristic of mesoporous materials [31] with a broad distribution of pore sizes (Fig.5). It must be noted that the calcined Cu-Fe-HTs reveals the formation of finer hysteresis loops whose volume decreases with the increase of the calcination temperature.

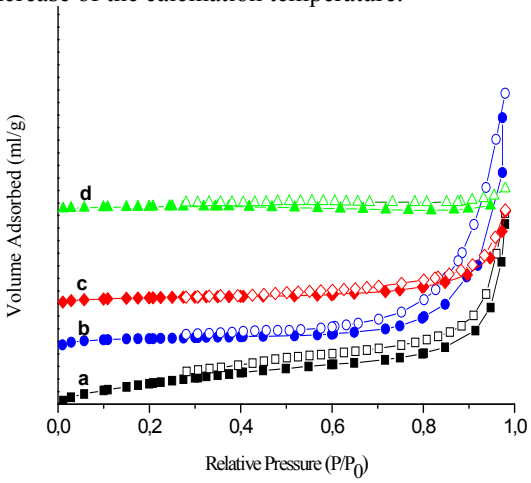


Fig.5. Nitrogen adsorption–desorption isotherms for (a) Cu-Fe-LDH, (b) Cu-Fe-400, (c) Cu-Fe-600 and (d) Cu-Fe-800

The morphology of the Cu-Fe-LDH and the precursors calcined were revealed by SEM and is shown in Fig.6. Cu-Fe-LDH showed a flower-like hierarchical morphology typical of LDH (Fig. 6a), similar shapes were obtained by Gennequin et al. [32]. Fig. 6b shows denser and more closely packed microstructure than Fig. 6a, these result reveal that the change in the solid structure after heat treatment at 400°C. In contrast, the Cu-Fe-600 consists of many irregular spherical grains of different colours; these observations confirm the formation of oxide mixture (Fig.6c). On the other hand, the Cu-Fe-800 in Fig. 6d shows an agglomerated morphology of homogeneity particle size and color, in accordance with the XRD results, shows that with increase in the calcinations temperature causes an increase in particle size.

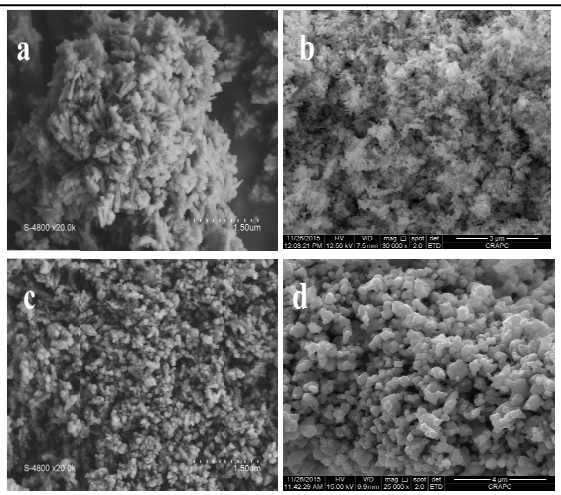


Fig. 6. SEM images for (a) Cu-Fe-LDH, (b) Cu-Fe-400, (c) Cu-Fe-600 and (d) Cu-Fe-800

3.2 Catalytic Activity/Selectivity

Benzaldehyde, with its aromatic ring, was used as a model molecule to study the hydrogenation of aldehydes. Catalytic activity over different catalytic systems was evaluated using a fixed-bed at atmospheric pressure and hydrogen-reducing pretreament for 2 hours. The catalytic performance of catalysts sensitive on both reaction temperature and the nature of oxides formed after the heat-treatment. The observed products for the benzaldehyde hydrogenation are benzyl alcohol (BOL), toluene (TOL) and benzene (BENZ).

3.2.1 Activity of Cu-Fe catalysts

The benzaldehyde conversion as a function of temperature over the different catalytic systems was presented in Fig.7 and Fig.8. The catalytic performance of catalysts sensitive on both reaction temperature and the nature of oxides formed after the heat-treatment.

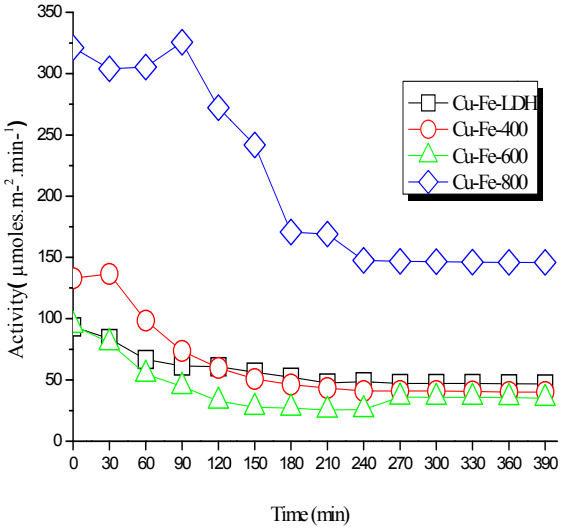


Fig. 7. Conversion of benzaldehyde with time on stream at 100°C under H_2 flow for the for (a) Cu-Fe-LDH, (b) Cu-Fe-400, (c) Cu-Fe-600 and (d) Cu-Fe-800 catalysts. Pre-treatment: H_2/350°C

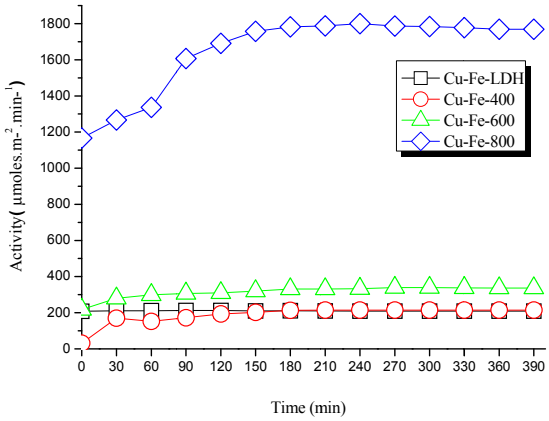


Fig. 8. Conversion of benzaldehyde with time on stream at 200°C under H_2 flow for the for (a) Cu-Fe-LDH, (b) Cu-Fe-400, (c) Cu-Fe-600 and (d) Cu-Fe-800 catalysts. Pre-treatment: H_2/350°C

The data in Table 3 were recorded in steady-state. The results show that the conversion increases with increasing of the reaction temperature from 100 to 200°C, and the highest activity was observed at 200°C for all precursors (Fig.8). At low reaction temperature (100°C), catalysts exhibited initial deactivation before the steady-state was established and the metal oxides formed from the heat treatment of Cu-Fe-LDH react less at low reaction temperature (Fig.7). We suggested that, equilibrium adsorption /desorption is reached only after 4 hours of reaction. Much higher conversion was obtained at 200°C for all catalysts. On the other hand, the maximum of conversion was observed at 200°C for Cu-Fe-800 (Fig.8). Indeed, the decrease of reaction temperature plays an important role in the adsorption of the reactant and release from the active site.

Catayst	T (°C)	A_i[a] ($\mu moles.m^{-2}.min^{-1}$)	Selectivity[a] (%) Benzyl alcohol	Toluene	Benzene
Cu-Fe-LDH	100	61,0	100	-	-
	200	211,0	64	32	4
Cu-Fe-400	100	63,1	100	-	-
	200	189,4	94	6	-
Cu-Fe-600	100	69,0	100	-	-
	200	247,0	76	24	-
Cu-Fe-800	100	280,0	100	-	-
	200	1685,0	60	39	3

Table.3 Catalytic results for gas phase hydrogenation of benzaldehyde over the Cu/Fe catalysts

[a]Steady-state activity and selectivity measured after 90 min of reaction time.

On the other hand, the highest activity obtained over Cu-Fe-800, may be explained by the formation of large particles size of the metal oxide and the presence of spinel $CuFe_2O_4$ after heat treatment at 800°C. It is well known from literature that the catalytic activity of the spinel ferrites depends upon various factors like particle size, redox properties of metal ions and their distribution among tetrahedral sites and octahedral sites of the cubic spinel lattice [33]. In ferrites [34,35], the metal ions present in the octahedral sites play a crucial role in catalysis.

This is due to the fact that octahedral sites are exposed on the surface. Moreover, metal ions at

octahedral sites are placed at larger distances so as to interact freely with the reactant molecules. Therefore, the catalytic activity of the spinel ferrite was highest because of the presence of both Cu^{2+} and Fe^{3+} ions in the octahedral sites of the ferrite sub-lattice. Due to this, there is transfer of electron between Cu^{+}-Cu^{2+} and Fe^{2+}-Fe^{3+} ion pairs [36], which enhances its catalytic activity.

3.2.2. Selectivity and reaction mechanism

Benzyl alcohol is the only observed product on all catalysts at low reaction temperature (100°C). The increasing the calcination temperature does not affect the selectivity of benzyl alcohol. At 200°C, the selectivity to benzyl alcohol decreases on the calcined solids. The increase in calcinations temperature leads to increases of selectivity, the most important and remarkable selectivity in benzyl alcohol (94%) obtained on the Cu-Fe-400 catalyst (table 3).

The high activities of the oxide phases formed from the Cu-Fe-LDH system for the benzaldehyde hydrogenation to alcohol, in spite of relatively low specific surface areas of the calcined systems (from 17 and 3 m^2/g, are may be consistent with the high activity of copper towards the selective hydrogenation of the C=O bond [37]. The active site in copper catalyzed hydrogenation reactions is the association of Cu(I) in an octahedral environment with hydride ion ($Cu^{\delta+}$-$H^{\delta-}$). The ionic character of the site can explain the strong reactivity toward the highly polarized C=O bond but also with the C-O bond of the alcohol product and, as a consequence, the competitive adsorption between the reactant and product. In addition, the presence of Fe in the LDH structure leads to a significant increase of selectivity. The obtained high benzyl alcohol selectivity over Cu/Fe calcined precursor is probably related to the iron redox properties and/or acid-base sites of Fe-O sites formed after calcination of the Cu-Fe-HDL precursor which leads an increase of C=O bond polarization and facilitate the dissociation of hydrogen (Fe(H)-O(H)).

The reaction mechanism of the benzyl alcohol formation from benzaldehyde could occur via a 1-2 nucleophilic addition, where the carbonyl function is activated on the active site.¶ Benzaldehyde adsorption, where both the aromatic ring and carbonyl group are co-planar to the surface (Fig.9), can facilitate C=O polarization, rendering the oxygen susceptible to a nucleophilic attack with hydrogen surface species as active intermediates for the direct hydrogenation of benzaldehyde to benzyl alcohol [37,38].

Toluene is favoured at high temperature on all catalysts. The toluene formation is obtained at 200°C and high benzaldehyde conversion in the Cu-Fe-LDH system with for 32% of toluene selectivity. In the case of Cu-Fe-HTs calcined catalysts, the results show that toluene selectivity increases from 6 to 39% when calcinations temperature increases from 400 to 800°C (tableau 3), the benzyl alcohol selectivity decreases with the increasing of the toluene selectivity. The mechanism is believed to be a consecutive reaction of hydrogenolysis of benzylalcohol [37]. Also, one is allowed to think that toluene formation probably resulted in the extension of the alcohol function (O-H) on a Brönsted acid site followed by the hydrogenolysis of the protonated specie on an adjacent copper site (Fig.10) [39].

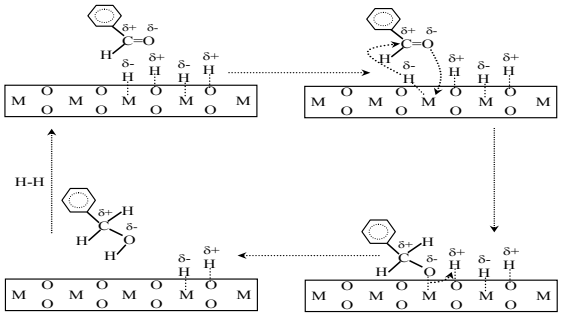


Fig.9 Reaction pathways of benzaldehyde hydrogenation to benzyl alcohol

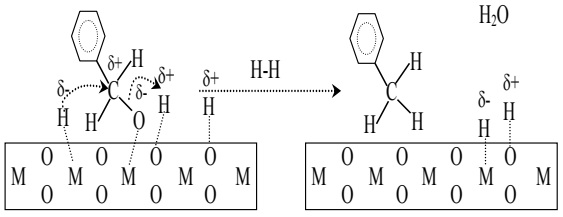


Fig.10 Reaction pathways of benzaldehyde hydrogenation to toluene

Benzene appeared only with the Cu-Fe-HDL (4%) and Cu-Fe-800 (3%) catalysts at 200 °C (Table 3) and it appears on the most active catalysts. This result was confirmed that benzene formation was produced directly from the reactant molecule and not from the alcohol or toluene intermediates, it was suggested that the benzene formation process is a decarbonation on the Bronsted acid sites [40] and that benzene would be considered as the product of the hydrogenolysis of the external C–C bond of benzaldehyde (Fig.11). Gas phase kinetic studies on the benzaldehyde conversion over platinum [41] or nickel [42] catalysts showed that benzene was produced directly from the reactant molecule and not from the alcohol or toluene as intermediates. It can also be produced via toluene hydrodealkylation [40] with the formation of methane in parallel.

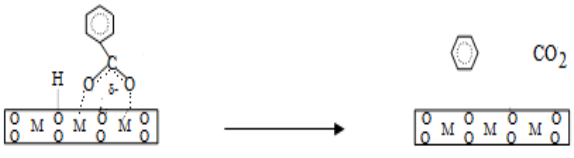


Fig.11 Reaction pathways of benzaldehyde hydrogenation to benzene

IV. CONCLUSION

In this study, Cu-Fe-LDH and Cu/Fe calcined exhibited good catalytic activity for the hydrogenation of benzaldehyde to benzyl alcohol. This high catalytic performance would be due to the combination of iron and copper species that have acid-base and/or redox properties of Fe-O sites formed after calcination. Toluene formation can result from the subsequent conversion of the alcohol and benzaldehyde hydrogenolysis and benzene from benzaldehyde decarbonation over the acid sites.

ACKNOWLEDGEMENTS

The authors wish to greatly thank Didier Tichit, Géradine Layrac and Thomas Cacciaguerra from Charles Gerhardt Institute (Matériaux Avancés pour la catalyse et la santé, CNRS, Montpelier, France) for their precious technical help (XRD, TEM, SEM-EDX, TGA-DTG and BET experiments).

REFERENCES

[1] Z. P. Xu, G.Q. Lu, Chem. Mater. Vol.17, pp 1055, 2005
[2] R. E. Johnsen, P. Norby, J. Phys. Chem. C. Vol. 113, pp 19061, 2009
[3] G. Pan, Z. Ni, F. Cao, X. Li, Appl. Clay Sci. Vol. 58, pp 108, 2012
[4] H.S. Panda, R. Srivastava, D. Bahadur, J. Phys. Chem. C. Vol. 113, pp 9560, 2009
[5] G.R. Williams, A.I. Khan, D. O'Hare, Struct. Bond. Vol. 119, pp 161, 2006
[6] D.G. Evans, R.C.T. Slade, Struct. Bond. Vol. 119, pp 1, 2006
[7] G.R. Williams, T.G. Dunbar, A. J. Beer, A. M. Fogg, D. O'Hare, J. Mater. Chem. Vol. 16, pp 1222, 2006
[8] W. Shi, S. He, M. Wei, D.G. Evans, X. Duan, Adv. Funct. Mater. Vol. 20, pp 3856, 2010
[9] Q. Li, H. Yi , X. Tang, S. Zhao, B. Zhao, D. Liu, F. Gao, Chem Eng J. Vol. 284, pp 103, 2016
[10] X.Y. Yu, T. Luo, Y. Jia, R.X. Xu, C. Gao, Y.X. Zhang, J.H. Liu, X.J. Huang, Nanoscale. Vol. 4, pp 3466, 2012
[11] C. Gao, X.Y. Yu, T. Luo, Y. Jia, B. Sun, J.H. Liu, X.J. Huang, J. Mater. Chem. A. Vol. 2, pp 2119, 2014
[12] D. Shan, S. Cosnier, C. Mousty, Biosens. Bioelectron. Vol. 20, pp 390, 2004
[13] H. Zazoua, A. Boudjemaa, R. Chebout, K. Bachari, Int. J. Energy. Res. Vol. 38, pp 2010, 2014
[14] H. Zazoua, A. Saadi, K. Bachari, D. Halliche, C. Rabia, Res. Chem. Intermed. Vol. 40, pp 931, 2014
[15] H.U. Blaser, A. Indolese, A. Schnyder, H. Steiner, M. Studer, J. Mol. Catal. A Chem. Vol. 173, pp 3, 2001
[16] J. Jenck, J.E. Germain, J Catal. Vol.65, pp 141, 1980
[17] D. Divakar, D. Manikandan, G. Kalidoss, T. Sivakumar, Catal Lett. Vol.125, pp 277, 2008
[18] H.A. Zahalka, H. Alper, Organometallics. Vol. 5, pp 1909, 1986
[19] R.H. Mitchel, Y.H. Lai, Tetrahedron Lett. Vol.21, pp 2637, 1980
[20] G M. Intille, U S Patent 4067900, 1975
[21] P. Gallezot, D. Richard, Catal Rev Sci Eng. Vol.40, pp 81, 1998
[22] V. Gutierrez, M. Alvarez, M.A. Volpe, Appl. Catal. A: Gen. Vol.413, pp 358, 2012
[23] W.T. Reichle, J Catal,Vol.94, pp 547, 1985
[24] F. Cavani, F. Trifiro, A. Vaccari, Catal. Today. Vol.11, pp 173, 1991
[25] V. Rives, Mater. Chem. Phys. Vol.75, pp 19, 2002
[26] P. Kustrowski, D. Sulkowska, L. Chmielarz, A. Rafalska-Lasocha, Mesoporous. Mater. Vol.78, pp 11, 2005
[27] J. Das, D. Das, G.P. Dash, M.K. Parida, J. Colloid. Interface Sci. Vol.251, pp 26, 2002
[28] M. Jitianu, M. Balasoiu, R. Marchidan, M. Zaharescu, D. Crisan, M. Craiu, Intern. J. Inorg. Mater. Vol.2, pp 287, 2000
[29] M. Dixit, M. Mishra, P.A. Joshi, D.O. Shah, J. Indus. Engin. Chem. Vol. 19, pp 458, 2013
[30] X. Han , K. Fang, J. Zhou , L. Zhao , Y. Sun, J. Coll. Inter. Sci. Vol. 470, pp 162, 2016
[31] IUPAC Reporting physisorption data for gas/solid system, Pure Appl. Chem. Vol.57, pp 603, 1985
[32] C. Gennequin, T. Barakat, H.L. Tidahya, R. Cousin, J.-F. Lamonier, A. Aboukaı¨s, S. Siffert, Catal. Today. Vol.157, pp 191, 2010
[33] M. Kooti, M. Afshari, Sci . Iran. Vol.19, pp 1991, 2012
[34] A.Goyal, S. Bansal, S. Singhal, Int. J. Hydrogen. Energy. Vol.39, pp 4895,2014
[35] J. Feng, L. Sua, Y. Ma, C. Ren, Q. Guo, X. Chen, Chem. Eng. J. Vol.221, pp 16, 2013
[36] E. Casbeer, VK. Sharma, XZ. Li, Sep. Purif. Technol. Vol.87, pp 1, 2012
[37] K. Lanasri, A. Saadi, K. Bachari, D. Halliche, O. Cherifi, Stud. in Surf. Sci and Catal. Vol.174, pp 1279, 2008
[38] N. Haddad, A. Saadi, A. Löfberg, R. N. Vannier, E. Bordes-Richard E, C. Rabia, J. Mol .Catal. A Chem. Vol.396, pp 207, 2015
[39] A.Saadi, Z. Rassoul, M.M. Bettahar, J. Mol. Catal. A Chem. Vol.164, pp 205, 2000
[40] A. Ausavasukhi, T. Sooknoi, D.E. Resasco. J. Catal. Vol.268, pp 68, 2009
[41] M.A. Vannice, D. Poondi D, J. Catal. Vol.169, pp 166, 1997
[42] M.A. Keane, Appl . Catal A Gen. Vol.118, pp 261, 1997

★★★